

# Oxidative conversion of propane over lithium-promoted magnesia catalyst II. Active site characterization and hydrocarbon activation

L. Leveles,<sup>a</sup> K. Seshan,<sup>a</sup> J.A. Lercher,<sup>b</sup> and L. Lefferts<sup>a,\*</sup>

<sup>a</sup> Faculty of Chemical Technology, University of Twente, Postbus 217, 7500 AE, Enschede, The Netherlands

<sup>b</sup> Institute for Chemical Technology, Department of Chemistry, Technische Universität München, Lichtenbergstrasse 4, D-85747 Garching, Germany

Received 9 October 2002; revised 26 February 2003; accepted 7 March 2003

## Abstract

Activation of propane over Li/MgO catalyst has been investigated. It is shown that a small fraction of the oxygen ions in Li/MgO catalysts can be removed from the catalyst by reduction treatment in H<sub>2</sub> at 600 °C. Catalytic activity of Li/MgO exhibits a strong correlation to the amount of oxygen that is removed. It is proposed that the sites containing removable oxygen are responsible for the activation of propane. About 70 propane molecules were converted after consumption of one such oxygen site, in the absence of gas-phase oxygen, implying a mechanism in which propane molecules are activated on the catalyst resulting in propyl radicals that are released to the gas phase where they undergo chain propagation reactions, resulting in the products observed. The active O site is consumed by conversion into an OH group, as the oxygen is not removed from the catalyst with propane. The oxidative conversion of propane over Li/MgO catalysts follows a mixed heterogeneous-homogeneous radical chemistry where the catalyst acts as an initiator. At low propane partial pressures (0.1 bar), the catalyst surface area to volume ratio of the catalytic reactor does not influence the chain length in the propagation step. At higher propane partial pressures (> 0.3 bar), favoring extensive gas-phase reactions, the catalyst affects conversion and selectivity also via quenching and chain termination.

© 2003 Elsevier Inc. All rights reserved.

**Keywords:** Li/MgO; Alkanes oxidative dehydrogenation; Propene; Propylene; Ethene; Ethylene

## 1. Introduction

Oxidative conversion of alkanes to olefins, especially dehydrogenation propane to propene, has been and continues to be an important research subject. Despite the efforts, most of the redox-type catalyst systems reported in the literature gave low yields of propene (< 30%) due to combustion of propene to carbon oxides. On the other hand, nonredox catalysts such as Li-promoted magnesia resulted in olefin yields in the range of 50%, as a mixture of ethene and propene [1,2]. Although there are only a few studies of propane oxidative conversion, propane selective oxidation without use of a catalyst appears to produce better olefin selectivities than catalytically. Burch and Crabb [3] compared catalytic and noncatalytic performances of propane oxidative conversion and concluded that the combination of heterogeneous and homogeneous reactions offers a better

opportunity for obtaining commercially acceptable yields of olefins than a purely catalytic reaction. It is unclear from the literature whether noncatalytic contributions are important during catalytic propane conversion, unlike in methane oxidative coupling where the role of catalytic and homogeneous reactions is well established [4,5]. Some authors explain their results of propane conversion to olefins in terms of catalytic reactions only, without taking into account possible homogeneous gas-phase contribution [6–8], while others describe their results in terms of radical reactions in the gas-phase initiated on the catalyst, and radical-surface interactions [9,10].

In the preceding paper (part I) we have suggested a reaction mechanism that involves a sequence in which propane is first activated on the [Li<sup>+</sup>O<sup>-</sup>] active sites of Li/MgO catalysts. The resulting radical then desorbs and initiates a gas-phase chain propagation reaction. The conditions under which catalytic activation prevails over homogeneous activation were also defined [11]. It was observed that at low propane partial pressures catalytic activation prevails, while

\* Corresponding author.

E-mail address: [l.lefferts@utwente.nl](mailto:l.lefferts@utwente.nl) (L. Lefferts).

Table 1  
Chemical compositions and specific surface areas of the catalysts used

Catalyst	Composition	MgO (wt%)	Li <sub>2</sub> O (wt%)	Dy <sub>2</sub> O <sub>3</sub> (wt%)	BET (m <sup>2</sup> /g)
MgO	MgO	100	–	–	75.1
MgO (high surface area)	MgO	100	–	–	110
1%Li <sub>2</sub> O/MgO	MgLi <sub>0.007</sub> O <sub>x</sub>	99.0	1.0	–	11.4
3%Li <sub>2</sub> O/MgO	MgLi <sub>0.08</sub> O <sub>x</sub>	97.0	3.0	–	2.9
3%Li <sub>2</sub> O/MgO (high surface area)	MgLi <sub>0.08</sub> O <sub>x</sub>	97.0	3.0	–	6.2
7%Li <sub>2</sub> O/MgO	MgLi <sub>0.2</sub> O <sub>x</sub>	93.0	7.0	–	1.3
12%Li <sub>2</sub> O/MgO	MgLi <sub>0.37</sub> O <sub>x</sub>	88.0	12.0	–	< 1
Li/Dy/MgO	MgLi <sub>0.2</sub> Dy <sub>0.02</sub> O <sub>x</sub>	85	7.7	7.3	1.3
Li/Dy/MgO (high surface area)	MgLi <sub>0.2</sub> Dy <sub>0.02</sub> O <sub>x</sub>	85	7.7	7.3	6

at high partial pressures of propane (typically above 0.3 bar) homogeneous activation of propane contributes to the overall performance. The product spectrum was explained in terms of heterogeneously initiated radical-chain propagation reactions. The catalyst appears to contribute also via quenching of radicals; however this effect was found to be significant only when radical concentrations are high at high partial pressures of propane (> 0.4 bar). The catalytic activation of propane has been proposed as the initiation step of the radical chemistry. Oxygen of the [Li<sup>+</sup>O<sup>-</sup>] active site abstracts a hydrogen atom from propane, resulting in the formation of *n*- or isopropyl radicals. These radicals are released into the gas phase where they first undergo decomposition reactions. The two types of propyl radicals have different decomposition routes: isopropyl gives propene and a hydrogen radical, and *n*-propyl gives ethene and a methyl radical. The radicals that result from the decomposition continue the chain propagation reactions, by activating new propane molecules resulting in a quasi-equal distribution of iso- and *n*-propyl radicals. In the presence of oxygen the concentration of radicals increases because oxygen reacts fast with the propyl radicals to form propene and a new chain-carrier radical, HO<sub>2</sub>•. Methyl radicals are converted either to methane at low partial pressures of oxygen or to CO when the oxygen partial pressure is relatively high [11].

We reported earlier on the effect of the catalyst constituents and the role of chlorine in a Mg–Li–Dy–Cl–O complex catalyst [2,12]. It was concluded that only Li is crucial in magnesia-based catalysts for the catalyst activity and selectivity; moreover, chlorine introduced stability problems.

The aim of this paper is to characterize the active sites of Li-promoted magnesia catalysts that are responsible for the catalytic activation of propane, and to describe the role of Li in creating these active sites. All measurements reported here were carried out using a low propane partial pressure (0.1 bar) so that homogeneous activation of propane is not significant, unless otherwise noted.

## 2. Experimental

Catalysts containing varying amounts of Li, studied in this paper, were prepared from MgO (Merck, assay 99.6%; high surface area magnesia from Ube Mat. Ind. 99.98%)

and LiNO<sub>3</sub> (Merck, > 98.0%) and for dysprosia-containing catalyst Dy<sub>2</sub>O<sub>3</sub> (Fluka, 99.9%), according to the wet impregnation method described in detail in [2]. The Li content and the concentrations of impurities in both the bulk and the surface of the samples were determined with XRF (Philips PW1480) and XPS (Physical Instruments Φ Quantum 2000), respectively. The bulk compositions and surface areas of the catalysts studied are presented in Table 1.

Sorption measurements were carried out with a Mettler-Toledo TGA-SDTA apparatus. Argon was used as the carrier gas. Typically, 50 to 100 mg of catalyst was used in a 70-μl alumina crucible, using a gas flow rate of 50 ml/min. The samples were activated at 750 °C in Ar until a constant weight was measured. Gas mixtures with 10% reactive gas (CO<sub>2</sub>, O<sub>2</sub>, H<sub>2</sub>, or propane) in 90% Ar were used.

Steady-state catalytic measurements were carried out in a quartz microreactor (internal diameter 4 mm) under plug flow conditions at atmospheric pressure. The catalyst bed was packed between two quartz-wool plugs. Quartz inserts of 3 mm diameter were introduced on top and below the catalyst bed to minimize the empty volume. Further details involved in the preparation of catalysts, their characterization, and reaction rate measurements are reported elsewhere [2,11]. During transient catalytic measurements samples were collected using a multiport valve to store samples for later GC analysis. During pulse measurements the reactor effluent was directly connected via a Porapak Q column to the TCD detector.

## 3. Results

### 3.1. Catalytic performance of Li/MgO catalysts with varying Li content

In an earlier paper we have shown that the catalyst formulation can be simplified from a complex catalyst composition [Li–Cl–Dy–Mg–O] proposed in the patent literature [13], to [Mg–Li–O] only, without importantly affecting the catalyst performance [2]. Here we present a detailed study on how the Li content of the Li/MgO catalyst influences the activity and selectivity to the various products.

Table 2 presents the catalytic performance data for the catalysts with varying amounts of Li at several temperatures.

Table 2  
Performance of Li/MgO catalysts

Catalyst	T (°C)	Conversion (%)	Selectivity (%)			
			C <sub>3</sub> H <sub>6</sub>	C <sub>2</sub> H <sub>4</sub>	CH <sub>4</sub>	CO <sub>x</sub>
MgO	550	4.3	14.0	13.9	0.7	71.4
	600	11.1	24.7	26.8	2.5	46.0
	650	43.3	34.6	32.9	11.7	20.3
1%Li <sub>2</sub> O/MgO	550	7.6	22.2	18.0	0.6	59.2
	600	33.2	25.2	31.2	3.0	39.7
	650	64.1	19.7	36.2	7.6	32.5
3%Li <sub>2</sub> O/MgO	550	5.4	23.5	19.5	0.7	56.2
	600	25.1	30.2	31.5	3.2	34.2
	650	58.8	23.2	36.5	7.2	28.7
7%Li <sub>2</sub> O/MgO	550	1.2	28.4	28.2	2.2	41.0
	600	8.7	39.9	32.9	5.5	20.4
	650	33.1	34.9	36.7	8.1	16.6
12%Li <sub>2</sub> O/MgO	550	1.1	30.2	22.6	1.6	45.6
	600	7	43	32	5.3	18
	650	26.2	37.6	38.0	9.1	10.5

Conditions: 10% propane, 8% oxygen in He; 100 mg catalyst;  $\text{WHSV}_{\text{propane}}, 0.9 \text{ h}^{-1}$ ; total flow rate, 10 ml/min.

Conversion was the highest for the 1 wt% Li<sub>2</sub>O-containing catalyst at all temperatures. Selectivities to olefins generally increased with Li content but at 600 °C the selectivity for propene increased the most remarkably, from 25 to 40% when Li content increased from 0 to 7 wt% Li<sub>2</sub>O.

The activity of 1% Li<sub>2</sub>O/MgO catalyst was higher than the activity of MgO though the surface area of MgO was reduced considerably by Li addition (see Table 1). Addition of more Li further reduced the surface area paralleled by a decrease of the catalytic activity. Addition of Li to MgO had the most significant effect on activity at 600 °C, i.e., conversion increased three-fold by adding 1 wt% Li<sub>2</sub>O. Therefore, 600 °C has been chosen for more detailed studies.

Rate of propane conversion, at 600 °C, expressed in moles per gram catalyst per second (Fig. 1), showed an optimum at 1 wt% Li<sub>2</sub>O content. When the conversion rate of propane was expressed in moles per square meter catalyst per second, the rate increased with Li<sub>2</sub>O content up to 3 wt% where it leveled off.

In Fig. 2 the effect of Li content on the selectivities to the main products is shown for a fixed temperature (600 °C) at the same level of conversion (10%) achieved by space velocity variation. Propene selectivity increased continuously up to 7 wt% Li<sub>2</sub>O and remained constant up to 12 wt% Li<sub>2</sub>O. Ethene selectivity appeared to be constant for all the catalysts containing Li, and it was higher than that over pure MgO. Selectivities to CO and CO<sub>2</sub> were decreased strongly by increasing the Li content, whereas methane selectivity was slightly increased. All selectivities were similar for the catalysts containing 7 and 12 wt% Li<sub>2</sub>O.

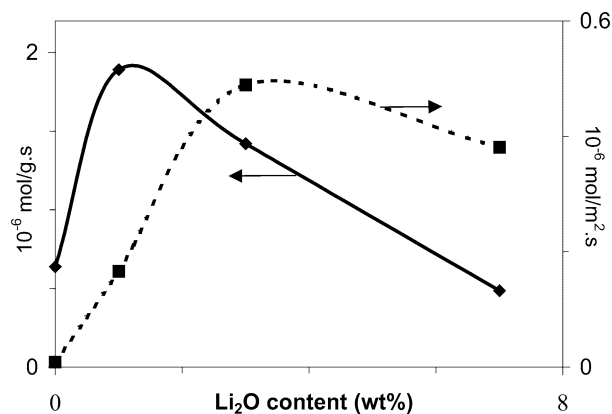


Fig. 1. Rate of conversion of propane over Li/MgO catalysts as a function of the Li content expressed as rates normalized to the catalyst weight and specific surface area, respectively. Conditions: 10% propane and 8% oxygen in He; T, 600 °C; total flow 10–80 ml/min.

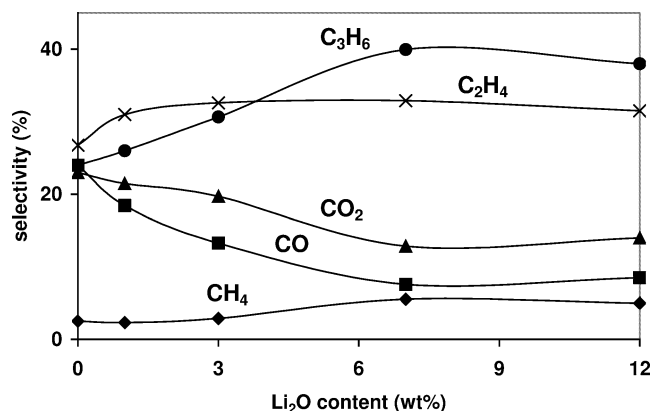


Fig. 2. Selectivities toward the main products over Li/MgO catalysts as a function of the Li content at 10% conversion. Conditions: 10% propane and 8% oxygen in He; T, 600 °C; total flow 10–80 ml/min.

### 3.2. Interaction of reactants and products on Li/MgO

Interaction of H<sub>2</sub>, O<sub>2</sub>, propane, and CO<sub>2</sub> with the Li/MgO catalysts was studied by sorption/desorption experiments in a TGA apparatus under reaction conditions (600 °C).

It was observed that treating the samples in hydrogen for at least 1 h at 600 °C or higher temperatures resulted in a considerable weight loss. After purging in Ar and admission of oxygen over the sample, the original weight of the sample was recovered instantaneously. It was concluded that oxygen from the sample was removed by hydrogen treatment and replenished upon oxygen treatment. The results of the measurements are presented in Table 3. The degree of deoxygenation, expressed as percentage of bulk oxygen, first increased and then decreased with increasing Li content. When we express the amount of removed oxygen as percentage of the total surface oxygen (calculated using the BET surface area and assuming (001) MgO surface) the deoxygenation degree increased with Li content up to 3 wt% Li<sub>2</sub>O where it leveled off with further increase of the Li content.

Table 3

The degree of deoxygenation of the Li/MgO catalysts measured by the weight loss during 1 h H<sub>2</sub> treatment and the weight gain upon subsequent oxygen admission; the amount of CO<sub>2</sub> sorbed and desorbed at 600 °C

Sample	Removed O expressed as			mol CO <sub>2</sub> desorbed/m <sup>2</sup> of catalyst	mol Li <sub>2</sub> O/g of catalyst	mol CO <sub>2</sub> sorbed/g of catalyst
	% of bulk oxygen	% of surface oxygen	mol/m <sup>2</sup> of catalyst			
MgO	0.02	0.48	7.46E-08	–	–	–
1%Li <sub>2</sub> O/MgO	0.10	14	2.24E-06	1.8E-06	3.3E-04	1.7E-04
3%Li <sub>2</sub> O/MgO	0.12	68	1.06E-05	7.9E-06	1.0E-03	6.4E-04
7%Li <sub>2</sub> O/MgO	0.05	62	9.70E-06	7.3E-06	2.3E-03	1.0E-03

Percentage of removed oxygen is calculated relative to the total oxygen in the samples and total surface oxygen assuming the (001) face of the MgO.

Oxidation and reduction of impurities may easily account for the weight changes observed. Therefore, the impurity level of all the Li/MgO catalysts and the starting materials used for the preparation of the catalysts were evaluated with XRF (only elements heavier than Na can be detected). The following compounds and elements were detected (maximum amount in wt% in parentheses): SiO<sub>2</sub> (0.2), S (0.06), Cl (0.05), K<sub>2</sub>O (0.002), CaO (0.04), Fe<sub>2</sub>O<sub>3</sub> (0.007), Cs<sub>2</sub>O (0.0002), BaO (0.003). MgO was the source of sulfur impurity, while iron was present in both MgO and LiNO<sub>3</sub>. XPS measurements showed no accumulation of any impurity on the surface; only Mg, O, C, and Li were detected on the surface of the catalysts.

Sorption/desorption of CO<sub>2</sub> was studied since the strong influence of CO<sub>2</sub> on the catalytic activity known from earlier work [11] makes CO<sub>2</sub> a suitable probe molecule for our catalysts. Switching CO<sub>2</sub> containing inert gas (Ar) to the samples in the TGA chamber resulted in a weight increase (Fig. 3). Switching off CO<sub>2</sub> from the gas stream resulted in a weight decrease of the samples; i.e., CO<sub>2</sub> desorbed partially (Fig. 3).

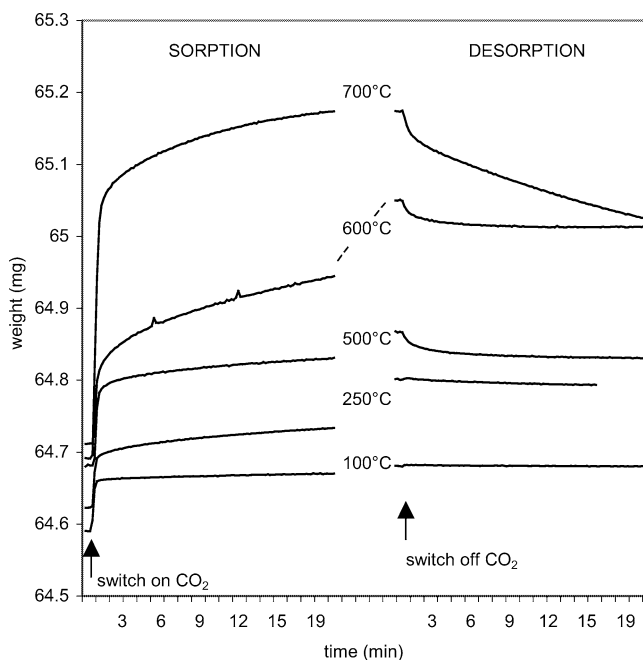


Fig. 3. Sorption and desorption curves measured in the TGA on the 1%Li<sub>2</sub>O/MgO catalyst. Conditions: 10% CO<sub>2</sub> in Ar; total flow, 50 ml/min.

Adsorption of CO<sub>2</sub> did not reach equilibrium within 20 min, except at 700 °C. Desorption equilibrated rapidly, except at 700 °C in which case the catalyst desorbed CO<sub>2</sub> continuously during measurement. At temperatures below 500 °C no significant desorption was observed.

At 600 °C CO<sub>2</sub> sorption/desorption measurements were also performed with samples containing varying amounts of Li. The results of these measurements are reported in Table 3. The quantity of sorbed CO<sub>2</sub> amounted roughly to half the amount of Li<sub>2</sub>O in moles, present in the catalyst. It must be noted also here that equilibrium was not reached during sorption measurements. It was further observed that the amount (in mol) of CO<sub>2</sub> that could be desorbed when switching from CO<sub>2</sub> to inert gas at 600 °C was in the same range as the number of moles of oxygen that could be removed with H<sub>2</sub>.

No propane adsorption was detected at the reaction temperature, i.e., 600 °C.

### 3.3. Influence of the deoxygenation degree on hydrocarbon activation

In order to investigate how the degree of deoxygenation influences the activity of the catalyst, two measurements were carried out using the same catalyst bed in a microreactor flow system at 600 °C. In the first measurement the catalyst was treated in 10% hydrogen for 1 h then purged for 10 min and finally a feed consisting of 10% propane in He was switched to the reactor. Immediately after the switch, samples were taken from the effluent stream and analyzed by GC. In the second measurement the sample was treated in hydrogen for 1 h followed by a brief oxygen treatment. After purging in He, 10% propane containing feed was admitted to the reactor. Samples were taken immediately after the propane admission and analyzed. Fig. 4 presents the conversion of propane obtained in these two experiments. The oxygen-treated catalyst produced 5 times higher conversions than the catalyst treated only in hydrogen. The oxygenated sample lost 80% of its original activity in 1 h.

In order to separate the propane reaction into redox reaction steps, reduction-oxidation cycles were attempted in pulse mode in the flow system at 600 °C. In the first experiment the catalyst bed was treated with 10% propane in He for 1 h. After purging in He for 10 min, pulses containing 10% oxygen in He were sent through the catalyst.

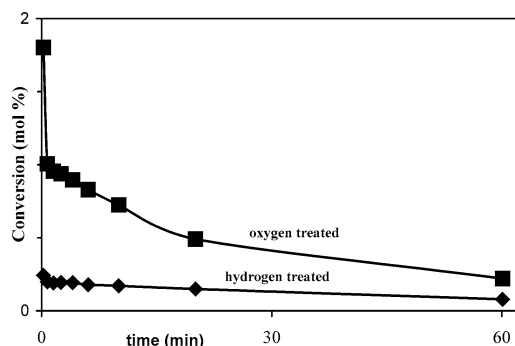


Fig. 4. Conversion of propane in the absence of oxygen over the oxygen-treated and hydrogen-treated catalyst. Conditions: 10% propane in He; total flow, 100 ml/min;  $T$ , 600 °C.

TCD Signal (arb. units)

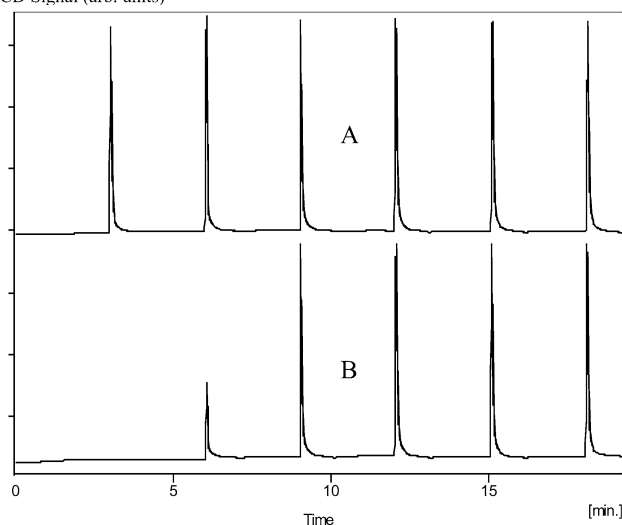


Fig. 5. TCD signal during oxygen pulsing of pretreated 1%Li<sub>2</sub>O/MgO catalyst at 600 °C. (A) Pretreatment in 10% propane, 1 h, 600 °C; (B) pretreatment in 10% H<sub>2</sub>, 1 h, 600 °C. Carrier (He) flow: 50 ml/min.

The pulses in the effluent stream were detected by thermal conductivity detector (TCD). The signal of the TCD in this experiment shown in Fig. 5A indicates no significant oxygen uptake after propane treatment. In the second experiment the catalyst was treated in hydrogen, and then the oxygen-containing pulses were sent through the reactor. The result of this experiment is presented in Fig. 5B. In contrast to the propane-treated catalyst, the catalyst treated in hydrogen consumed almost all oxygen from the first two pulses ( $\sim 10^{-6}$  mol O/m<sup>2</sup> catalyst).

### 3.4. Influence of the surface area on catalytic performance

In order to study the influence of surface area, high surface area MgO precursor was used to prepare catalysts with the same composition but higher surface area. The catalytic performances are presented in Table 4 for the 3% Li<sub>2</sub>O/MgO catalyst together with the BET surface areas and the concentration of sites that can be deoxygenated in H<sub>2</sub> at 600 °C. Increasing surface area from 3 to 6 m<sup>2</sup>/g had only

Table 4  
Dependence of conversion and selectivities on surface area, for Li/MgO catalyst

Catalyst	3%Li <sub>2</sub> O/MgO	
BET (m <sup>2</sup> /g)	3	6
Conversion (%)	10	10
Rate (10 <sup>-6</sup> mol g <sup>-1</sup> s <sup>-1</sup> )	2.8	3.0
(10 <sup>-6</sup> mol m <sup>-2</sup> s <sup>-1</sup> )	0.9	0.5
[Li <sup>+</sup> O <sup>-</sup> ] (10 <sup>-6</sup> mol/m <sup>-2</sup> )	11	5
	Selectivity (%)	
CH <sub>4</sub>	2.9	2.3
CO	13.3	20.9
CO <sub>2</sub>	19.7	21.1
C <sub>2</sub> H <sub>4</sub>	32.6	29.0
C <sub>3</sub> H <sub>6</sub>	30.7	26.3

Conditions: 600 °C; WHSV<sub>propane</sub>, 4.8 h<sup>-1</sup>; 10% propane and 8% O<sub>2</sub> in He; total flow, 40 ml/min; 100 mg catalyst.

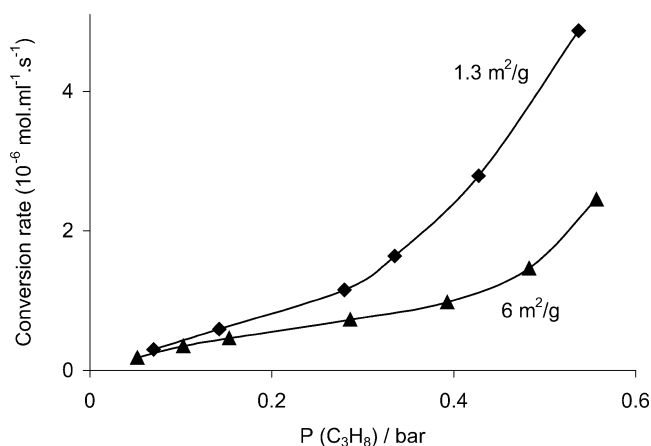


Fig. 6. Reaction rate of propane conversion vs propane partial pressure over two different catalysts with the same composition (Li/Dy/MgO) but different surface area. Conditions:  $P(\text{CO}_2)$ , 20 mbar;  $P(\text{O}_2)$ , 140 mbar;  $T$ , 600 °C; total flow, 100 ml/min.

marginal influence on the rate of conversion. However, selectivities to various products changed significantly from 3 to 6 m<sup>2</sup>/g. As a general trend, higher surface area resulted in lower olefin products selectivities and higher CO and CO<sub>2</sub> selectivities. Rate of propane conversion, calculated as moles per square meter catalyst per second, obviously resulted in a decrease of the activity by a factor of 2.

Catalysts with the same composition but different surface areas were prepared earlier by modifications of the preparation method (see [2] for details). Note, that these catalysts also include small amounts of dysprosia; however, the presence of dysprosia does not influence the product spectrum significantly [2]. The rate of propane conversion as a function of propane partial pressure measured under differential conditions (for details of measurement, see part I [11]) over two catalysts having the same composition but different surface areas is presented in Fig. 6. At low propane partial pressures ( $< 0.2$  bar) the two catalysts converted propane at a similar rate, whereas at high partial pressures ( $> 0.3$  bar)

propane converted about two times faster over the catalyst having lower surface area.

#### 4. Discussion

First, the role of Li in creating the active site will be discussed. Then, the mechanism of propane activation on the site created by Li and further reaction steps will be detailed.

##### 4.1. Role of Li in creating the active site with removable oxygen

The activity and selectivity increase with Li addition, as shown in Table 2 and Fig. 2, demonstrate the crucial role of Li in creating the active site: addition of up to 3 wt%  $\text{Li}_2\text{O}$  onto magnesia increases the rate of propane conversion normalized to catalyst surface area as shown in Fig. 1. The conclusion that Li is indispensable for creating active sites is in agreement with earlier statements. It was concluded from observations on the inhibition of the reaction by  $\text{CO}_2$  and from the interaction of the catalyst with  $\text{CO}_2$  in TPD experiments that Li is part of the active site. It was proposed that  $[\text{Li}^+\text{O}^-]$ -type active sites, as defects on the MgO surface, are responsible for catalytic activity, similarly to the methane oxidative coupling [12,14,15]. Furthermore, in the kinetic analysis of propane conversion, a strong correlation between catalytic activity and  $\text{CO}_2$  concentration was found, whereas it was shown that  $\text{CO}_2$  did not influence gas-phase reactions. It was proposed that  $[\text{Li}^+\text{CO}_3^-]$  is formed on the  $[\text{Li}^+\text{O}^-]$  active site based on the observation that  $\text{CO}_2$  showed a minus one order in the conversion rate of propane [11].

We attempt to quantify the concentration of  $[\text{Li}^+\text{O}^-]$  active sites by two methods. The first method consisted of removal of the oxygen from the active site and subsequent reoxidation, as shown in Fig. 5B. The surface concentration of removable oxygen is displayed in Table 3. The second method involved the decomposition of the unstable  $[\text{Li}^+\text{CO}_3^-]$ . The quantification of  $[\text{Li}^+\text{CO}_3^-]$  was made under conditions where it could be differentiated from  $\text{Li}_2\text{CO}_3$ , as follows. Fig. 3 shows two distinct modes of  $\text{CO}_2$  adsorption at 500 and 600 °C. The first mode of adsorption is irreversible at these temperatures and this is attributed to the formation of bulk  $\text{Li}_2\text{CO}_3$  from  $\text{Li}_2\text{O}$ . This conversion is rather slow and after 20 min the conversion of  $\text{Li}_2\text{O}$  is far from complete. Significant decomposition of the bulk  $\text{Li}_2\text{CO}_3$  phase is noted only at 700 °C. The second mode of adsorption is reversible, as part of the  $\text{CO}_2$  is desorbing when  $\text{CO}_2$  is removed from the gas phase at 500 or 600 °C. This is attributed to adsorption/desorption equilibrium of  $\text{CO}_2$  on  $[\text{Li}^+\text{O}^-]$  to form  $[\text{Li}^+\text{CO}_3^-]$ . This hypothesis is in agreement with the observation that the number of moles of desorbed  $\text{CO}_2$ , as the result of  $[\text{Li}^+\text{CO}_3^-]$  decomposition, is similar to the number of moles of removable oxygen at every Li content (Table 3). Further, the formation of  $[\text{Li}^+\text{CO}_3^-]$  is

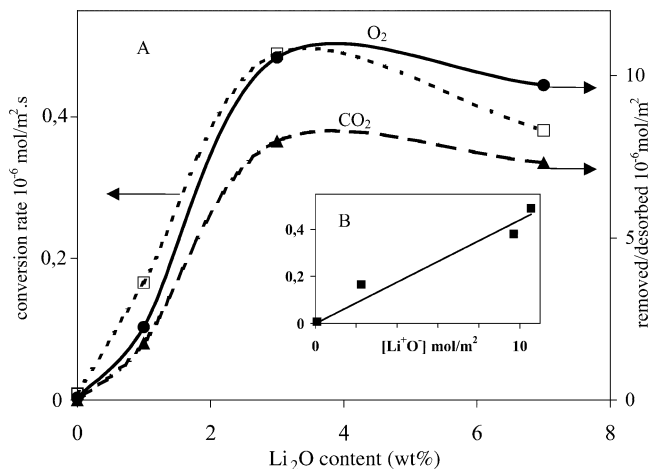


Fig. 7. Conversion rates related to the surface area (data from Fig. 1), deoxygenation degree (circles), and total  $\text{CO}_2$  desorbed (triangles) related to the surface (data from Table 3), for the Li/MgO catalysts vs the Li content at 600 °C (A); correlation of the activity with the density of active sites as measured by surface concentration of removable oxygen (B).

supported by the  $-1$  reaction order of  $\text{CO}_2$  observed during the kinetic measurements in part I of this publication. This implies that reversible adsorption of  $\text{CO}_2$  at 600 °C takes place on the same sites that can be reduced with  $\text{H}_2$  at 600 °C.

In summary, we consider the surface concentration of removable oxygen as well as the concentration of sites that adsorb  $\text{CO}_2$  reversibly at 600 and 500 °C as a measure for the concentration of  $[\text{Li}^+\text{O}^-]$  active sites. For further calculations we will use the concentration of active sites based on deoxygenation in  $\text{H}_2$  at 600 °C. The concentration of  $[\text{Li}^+\text{O}^-]$  species increases proportionally with the Li content up to 3 wt%  $\text{Li}_2\text{O}$ ; however, it is evident that only a small fraction of the available Li forms actually an active site (see Fig. 7A).

Catalytic activity is attributed to the removable oxygen present in the  $[\text{Li}^+\text{O}^-]$  site. This is demonstrated by the linear correlation of the reaction rates with the density of  $[\text{Li}^+\text{O}^-]$  sites (Fig. 7B). Further support for the claim that  $[\text{Li}^+\text{O}^-]$  activates propane is given by the low propane activation capacity of the deoxygenated catalyst (oxygen of the active site removed) compared to the fully oxygenated catalyst (Fig. 4) and the inhibition caused by  $\text{CO}_2$  adsorption on the  $[\text{Li}^+\text{O}^-]$  site, described in part I.

It is evident from the results that Li is not homogeneously distributed over the MgO surface: just 1 wt% of  $\text{Li}_2\text{O}$  would be sufficient to form four monolayers. Therefore, no further increase in activity should be expected with Li content. In contrast, Fig. 1 shows that catalyst activity increases with Li loading up to 3 wt%  $\text{Li}_2\text{O}$ . Apparently,  $\text{Li}_2\text{O}$  and MgO form a poorly defined mixture, which is also illustrated by the decrease of the surface area of the catalysts after calcination. Clearly, Li is not equally distributed over the surface of the catalyst, which agrees with claims in the literature that Li is present in clusters on the magnesia surface [16].

However, the question regarding the location of the  $[\text{Li}^+\text{O}^-]$  active site remains. Clusters of  $\text{Li}_2\text{O}$  on the  $\text{MgO}$  surface are not expected to show “redox” capacity, as observed here. In principle, only the presence of  $\text{Li}_2\text{O}_2$  phase under reaction conditions could account for oxygen release while forming  $\text{Li}_2\text{O}$ , as suggested in the literature [17,18]. However, the presence of such an unstable phase as  $\text{Li}_2\text{O}_2$  is arguable under the reaction conditions used, as it already decomposes below  $200^\circ\text{C}$ . In the references noted, the presence of the  $\text{Li}_2\text{O}_2$  phase was proposed based mainly on XRD data, but not unambiguously identified against other Li containing but more stable phases that can be present, e.g.,  $\text{LiOH}$ ,  $\text{LiOH}\cdot\text{H}_2\text{O}$ , and  $\text{Li}_2\text{CO}_3$ . Further, Bothe-Almquist et al. [17] used EPR evidence to argue for the presence of  $\text{Li}_2\text{O}_2$ , despite of the fact that  $\text{O}_2^{2-}$  in the peroxide is diamagnetic. Therefore, the presence of  $\text{Li}_2\text{O}_2$  is questionable, so is the role of this phase in the catalytic activity.

The oxygen removal/reoxidation is more conceivable in the case of a  $[\text{Li}^+\text{O}^-]$  defect on the  $\text{MgO}$  surface. This defect oxygen has peculiar properties, different from the rest of the lattice oxygen; it has, for example, EPR activity [19], and it was suggested to be removable under methane coupling conditions (see, for example, [20–22]).

The observed weight changes cannot be attributed to reduction and oxidation of impurities in the catalysts. The only elements present according to XRF analysis that may have introduced redox properties are Fe and S. If all the Fe present would undergo oxidation–reduction between  $\text{Fe}_2\text{O}_3$  and  $\text{FeO}$ , 0.0007 wt% change would be observed. In comparison, the measured samples showed much higher exchange capacity: 0.01 wt% for  $\text{MgO}$  and between 0.05 and 0.07 wt% for the  $\text{Li}/\text{MgO}$  catalysts in the reduction–oxidation cycles. In case sulfur is converted between sulfate and sulfite a max change of 0.03 wt% would result. However, none of the possible sulfites is stable above  $450^\circ\text{C}$ ; moreover, there was no sulfur found on the surface by XPS.

#### 4.2. Reaction mechanism of propane activation

It was shown in part I that the first propane molecule is activated on the catalyst and a propyl radical is released to the gas phase where it undergoes radical-chain propagation reactions. Activation of propane on the  $[\text{Li}^+\text{O}^-]$  active site takes place by splitting one C–H bond in propane while forming  $[\text{Li}^+\text{OH}^-]$  and a propyl radical that is released into the gas phase. Support for this mechanism is provided from the experiments presented in Fig. 5 where propane treatment did not result in oxygen removal from the catalyst. Thus, the removable oxygen of the active site is not removed during the activation of propane, nor it is eliminated in a subsequent dehydroxylation step. Product hydrogen concentration is too low (0.04 vol%) to be effective in oxygen removal.

Regeneration of the  $[\text{Li}^+\text{OH}^-]$  sites was proposed to occur upon oxygen admission, without the removal of the  $\text{O}^-$  of the active site [11]. However, under the pulsing conditions shown in Fig. 5A the reaction of oxygen with  $[\text{Li}^+\text{OH}^-]$  is

probably not sufficiently fast [23] to produce a noticeable oxygen uptake; nor could water evolution be confirmed due to detection difficulties.

Importantly, the amount of propane converted over the time on stream as shown in Fig. 4 is 70 times higher than the number of removable oxygen sites. This fact supports a radical-chain mechanism proposed in part I of this paper [11], in which one propane molecule is activated on the active site resulting in propyl radical which undergoes chain-propagation reactions in the gas phase. The number 70 is a typical chain-propagation length in homogeneous chemistry [24,25].

The surface area of the catalyst does not influence the chain length of the radical chain reaction at low propane partial pressures. This follows from the data in Table 4; two catalysts with the same number of active sites per gram show identical catalytic activity. Assuming that the activity per site is constant, despite the difference in the density of active sites in both catalysts, it follows that the rates of formation of radicals are identical. As the conversion rate did not change either, it must be concluded that the chain length is also constant. This is also supported by the low partial pressure data in Fig. 6 where catalysts with the same composition but differing surface area show similar activities. Further support for constant chain length is provided by the constant activity per active site for catalysts with varying surface areas. The variation of the surface area was induced by variation of Li loading, and activity vs active site concentration resulted in a linear relationship (Fig. 7B), indicating constant activity per site.

On the other hand the quenching role of the catalyst becomes important at high partial pressures of propane. From Fig. 6 it is observed that at high propane partial pressures the conversion rate of propane decreases with increased surface area. According to the proposed radical-chain mechanism, when increasing the partial pressure of propane, the concentration of radicals in the gas phase is expected to increase. When the concentration of radicals is higher, radical quenching is more efficient on the high surface area catalyst; thus, conversion is significantly decreased.

Increased  $\text{CO}_x$  selectivity with increased surface area (Table 4) indicates reaction pathways on the nonpromoted, unselective sites at the magnesia surface. Contribution to the increased  $\text{CO}_x$  selectivity could come partly from secondary reactions of olefins (only a small decrease in selectivity to olefins and corresponding increase in selectivity to  $\text{CO}_x$  was observed with increasing contact time/conversion of propane) and more efficient transformation of non-detectable oxygenated hydrocarbons to carbon oxides over the catalyst surface.

Selectivity and activity decrease due to interactions of radical intermediates with the catalyst surface were also reported earlier in the alkane oxidation literature [9,26,27] which agrees well with our suggestion. Simulations of surface initiated gas-phase reactions were also attempted; how-

ever modeling surface initiated gas-phase reactions is very complex and still needs further development [5,24,28]

## 5. Conclusions

It was confirmed that oxygen sites created by Li defects on MgO (noted as  $[\text{Li}^+\text{O}^-]$ ) activate the propane molecule via H $\cdot$  abstraction, based on the correlation between catalytic activity and active site density. The concentration of  $[\text{Li}^+\text{O}^-]$  sites was measured independently by  $\text{O}^-$  removal with  $\text{H}_2$  as well as by reversible  $\text{CO}_2$  adsorption at 600 °C.

The chain length of propagation reactions initiated on the catalyst is  $\sim 70$  in the absence of oxygen at 600 °C. During the initiation reactions the  $[\text{Li}^+\text{O}^-]$  site is transformed to  $[\text{Li}^+\text{OH}^-]$ . Regeneration of the active site does not require the oxygen removal by dehydroxylation. The surface area of the Li/MgO catalysts influences the chain length of the propagation reactions at high propane partial pressures only, due to quenching.

## Acknowledgments

This work was performed under the auspices of the Netherlands Institute for Catalysis Research (NIOK) and the Process-Technology Institute Twente (PIT). The financial support from STW Project No. 349-4428 is gratefully acknowledged. L. Leveles thanks Dr. I. Babich for help in TGA measurements.

## References

- [1] M.V. Landau, M.L. Kaliya, M. Herskowitz, P.F. van den Oosterkamp, P.S.G. Bocque, *Chemtech* 26 (1996) 24.
- [2] L. Leveles, S. Fuchs, K. Seshan, J.A. Lercher, L. Lefferts, *Appl. Catal. A: Gen.* 227 (2002) 287.
- [3] R. Burch, E.M. Crabb, *Appl. Catal. A* 100 (1993) 111.
- [4] M. Hatano, P.G. Hinson, K.S. Vines, J.H. Lunsford, *J. Catal.* 124 (1990) 557.
- [5] P.M. Couwenberg, Q. Chen, G.B. Marin, *Ind. Eng. Chem. Res.* 35 (1996) 3999.
- [6] O.V. Buyevskaya, M. Baerns, *Catal. Today* 42 (1998) 315.
- [7] W.D. Zhang, X.P. Zhou, D.L. Tang, H.L. Wan, K. Tsai, *Catal. Lett.* 23 (1994) 103.
- [8] Q.J. Ge, B. Zhaorigetu, C.Y. Yu, W.Z. Li, H.Y. Xu, *Catal. Lett.* 68 (2000) 59.
- [9] M.Y. Sinev, L.Y. Margolis, V.Y. Bychkov, V.N. Korchak, *Stud. Surf. Sci. Catal.* 110 (1997) 327.
- [10] I.M. Dahl, K. Grande, K.J. Jens, E. Rytter, A. Slagtern, *Appl. Catal.* 77 (1991) 163.
- [11] L. Leveles, K. Seshan, J.A. Lercher, L. Lefferts, *J. Catal.* (2003).
- [12] S. Fuchs, L. Leveles, K. Seshan, L. Lefferts, A. Lemonidou, J.A. Lercher, *Top. Catal.* 15 (2001) 169.
- [13] M. Herskowitz, M. Landau, M. Kaliya, *PCT Int. Appl. WO 9622161 A1* 25 July 1996.
- [14] T. Ito, J.X. Wang, C.H. Lin, J.H. Lunsford, *J. Am. Chem. Soc.* 107 (1985) 5062.
- [15] D.J. Driscoll, W. Martir, J.X. Wang, J.H. Lunsford, *Adv. Catal.* 35 (1987) 139.
- [16] D.J. Wang, M.P. Rosynek, J.H. Lunsford, *J. Catal.* 151 (1995) 155.
- [17] C.L. Bothe-Almquist, R.P. Ettireddy, A. Bobst, P.G. Smirniotis, *J. Catal.* 192 (2000) 174.
- [18] M.V. Landau, A. Gutman, M. Herskowitz, R. Shuker, Y. Bitton, D. Mogilyansky, *J. Mol. Catal. A: Chem.* 176 (2001) 127.
- [19] M. Che, A.J. Tench, *Adv. Catal.* 31 (1982) 77.
- [20] M.Y. Sinev, V.Y. Bychkov, *Kinet. Catal.* 34 (1993) 272.
- [21] V.R. Choudhary, V.H. Rane, S.T. Chaudhari, *React. Kinet. Catal. Lett.* 63 (1998) 371.
- [22] G.C. Hoogendam, PhD thesis, University of Twente, the Netherlands, 1996.
- [23] M.Y. Sinev, V.Y. Bychkov, *Kinet. Catal.* 40 (1999) 819.
- [24] C.A. Mims, R. Mauti, A.M. Dean, K.D. Rose, *J. Phys. Chem.* 98 (1994) 13357.
- [25] E. Ranzi, A. Sogaro, P. Gaffuri, G. Pennati, C.K. Westbrook, W.J. Pitz, *Combust. Flame* 99 (1994) 201.
- [26] V.P. Vislovskiy, T.E. Suleimanov, M.Y. Sinev, Y.P. Tulenin, L.Y. Margolis, V.C. Corberan, *Catal. Today* 61 (2000) 287.
- [27] M.Y. Sinev, L.Y. Margolis, V.N. Korchak, *Uspekhi Khimii* 64 (1995) 373.
- [28] M.Y. Sinev, *Catal. Today* 24 (1995) 389.